

Published in final edited form as:

*Appl Spectrosc.* 2012 June ; 66(6): 728–730. doi:10.1366/12-06592.

## Fluorocarbon Fiber-Optic Raman Probe for Non-Invasive Raman Spectroscopy

PAUL I. OKAGBARE and MICHAEL D. MORRIS\*

Department of Chemistry, University of Michigan, Ann Arbor, Michigan 48109-1055

### Abstract

We report the development of a novel fiber-optic Raman probe using a graded index fluorocarbon optical fiber. The fluorocarbon fiber has a simple Raman spectrum, a low fluorescence background, and generates a Raman signal that in turbid media serves as an intense reference Raman signal that corrects for albedo. The intensity of the reference signal can easily be varied as needed by scaling the length of the excitation fiber. Additionally, the fluorocarbon probe eliminates the broad silica Raman bands generated in conventional silica-core fiber without the need for filters.

### Index Headings

Fluorocarbon fiber; Cytos; Raman spectroscopy; Reference signal; Fiber-optic probe; Tissue albedo; Graded-index fiber; Non-invasive

---

Fiber probe Raman spectroscopy is widely used.<sup>1–3</sup> Several designs and configurations of optical fibers have been adopted for different applications.<sup>4–7</sup> Deep subsurface Raman spectroscopy became practical with the advent of spatially offset Raman spectroscopy<sup>8–12</sup> and transmission Raman spectroscopy.<sup>13</sup> These techniques have enabled depth-resolved probing and molecular characterization of various turbid media ranging from plastic containers to pharmaceuticals and even to human and animal tissues.<sup>14–16</sup> However, while the laser power exiting the distal end of an excitation fiber is easily measured, neither the albedo of a turbid material nor the scattering coefficients and geometry are known or easily measured in the field. Therefore, the power delivered to and propagating through the material is also uncertain.<sup>17–20</sup>

For example non-invasive Raman spectroscopy of human subjects or live animals requires the penetration of the interrogating laser through one or more layers of tissues that vary significantly in their diffuse reflectivity.<sup>21–23</sup> This variation in optical properties and albedo makes quantitative spectroscopy in turbid media difficult.<sup>23</sup> Thus, spectra normalization to a specific tissue component to extract quantitative information is accompanied by much uncertainty. The situation is different in spectroscopy of excised tissue specimens, where normalization to a tissue component band is feasible since light scattering in these specimens is surface weighted and can be neglected. For subsurface Raman spectroscopy of turbid media, a suitable Raman band that can be used as internal reference for spectral normalization is required.

A simple approach is to use an externally generated signal proportional to the laser intensity exiting the excitation fiber or fibers.<sup>24</sup> We previously reported the use of a fluorinated ethylene-propylene copolymer (FEP) cap on the excitation fiber to generate a reference Raman signal (C–F stretch,  $732\text{ cm}^{-1}$ ) that scales with the intensity of the laser light propagating through a turbid material.<sup>25</sup> The FEP cap can only be 2–3 mm long because FEP is flexible and long caps are subject to bending. Additionally, the FEP cap transmits fiber-generated silica Raman bands, which are broad and often difficult to remove from spectra.

A simpler approach is to generate a reference Raman signal using fluorocarbon-core excitation fiber(s). We report here on the use of a graded index fluorocarbon fiber probe with a polyperfluoro-butenylvinylether (Cytop) core. The Cytop Raman spectrum is similar to that of other fluorocarbons, although the C–F stretch appears at  $692\text{ cm}^{-1}$ .

For these experiments the previously reported instrument was used.<sup>25</sup> Briefly, it consists of a Raman spectrograph (Rxn1, Kaiser Optical Systems Inc., Ann Arbor, MI) and an external 830 nm laser (IO830MM0600MF-NL: #3142, Innovative Photonic Solutions, NJ). The overall fiber optic probe design is the same as previously reported. The custom-fabricated (FiberTech Optica, Kitchener, ON, Canada) fluorocarbon input fiber is shown in Fig. 1, along with its Raman spectrum and that of a conventional silica fiber. Laser propagation through the fiber generated the CF stretch at  $692\text{ cm}^{-1}$  and weaker bands at 1474, 1532, 1632, and  $1667\text{ cm}^{-1}$  (see Fig. 1B). The band intensities are proportional to the laser intensity propagating through the specimen (data not shown). Photon diffusion through the specimen can be defined by multiple collection fibers placed around the specimen. The intensity of the reference signal can be varied by varying the length of the excitation fiber. Normalization of collected Raman spectra to the Cytop reference signal provides quantitative information from subsurface Raman spectra of turbid media, as previously demonstrated using an FEP-capped excitation fiber.<sup>25</sup> The fluorocarbon excitation fiber also eliminates silica background and minimizes total silica contribution to collected Raman spectra.<sup>4</sup>

We demonstrate the generation of reference signals using a 5-meter excitation fiber and both a Delrin block and a phantom that models light propagation through and bone Raman spectroscopy of a rat tibia.<sup>25</sup> The 1.23-mm-diameter stainless steel ferrule at the distal end of the fiber is held in place with a custom-designed probe holder<sup>26,27</sup> and contacts the material under test.

The Raman spectrum of the phantom is shown in Fig. 2A. The polymer reference band at  $692\text{ cm}^{-1}$  is more intense than the hydroxyapatite (HAP)  $960\text{ cm}^{-1}$  band. A residual silica Raman signal, generated in the collection fibers, remains but is attenuated because there is no contribution from the excitation fiber. One major advantage of this new probe design is the simplicity of tuning the reference signal intensity as required by changing the length of the excitation fiber. Also, Raman measurement was carried out using our previously reported silica fiber probe for excitation.<sup>27</sup> The result from this measurement is shown in Fig. 2B. A careful inspection of the Raman data presented in Fig. 2 showed a decrease in silica background contribution to the spectra when the fluorocarbon fiber optic probe was used for excitation (Fig. 2A) compared to when the silica fiber probe was used for excitation (Fig. 2B). The broad silica background centered at  $\sim 800\text{ cm}^{-1}$  is more intense in the spectra acquired with the silica excitation fiber (Fig. 2B). The residual silica background seen in Fig. 2A is from the collection fibers, which are conventional multimode silica core fibers.<sup>4</sup>

A cylinder of Delrin was used as a simpler model (Fig. 3). As before, an intense  $692\text{ cm}^{-1}$  C–F band is generated in the excitation fiber (Fig. 3A), and the silica band is greatly

attenuated compared to the broad silica band at  $\sim 800\text{ cm}^{-1}$  in the Raman spectrum generated with a silica excitation fiber (Fig. 3B).

Of course, the fluorocarbon fibers can be used in many related fiber-optic probe configurations. For example, we have placed 1 to 2 meter lengths of commercially available fluorocarbon fibers with standard connectors between the exciting laser and silica collection fibers. The insertion loss is only about 10%. A suitable reference signal is generated, but silica background is larger than found with fluorocarbon excitation fibers alone.

## Acknowledgments

The authors acknowledge support of this work through National Institutes of Health grants R01AR055222 and R01AR056646.

## References

1. Chen P, Shen AG, Zhou XD, Hu JM. Bio-Raman spectroscopy: a potential clinical analytical method assisting in disease diagnosis. *Anal Methods*. 2011; 3(6):1257–69.
2. Utzinger U, Richards-Kortum RR. Fiber optic probes for biomedical optical spectroscopy. *J Biomed Opt*. 2003; 8(1):121–47. [PubMed: 12542388]
3. Motz JT, Hunter M, Galindo LH, Gardecki JA, Kramer JR, Dasari RR, Feld MS. Optical fiber probe for biomedical Raman spectroscopy. *Appl Opt*. 2004; 43(3):542–54. [PubMed: 14765912]
4. Sato, H.; Shinzawa, H.; Komachi, Y. Fiber-Optic Raman Probes for Biomedical and Pharmaceutical Applications. In: Matousek, P.; Morris, MD., editors. *Emerging Raman Applications and Techniques in Biomedical and Pharmaceutical Fields*. Springer; Berlin Heidelberg: 2010. p. 25-45.
5. Komachi Y, Sato H, Tashiro H. Intravascular Raman spectroscopic catheter for molecular diagnosis of atherosclerotic coronary disease. *Appl Opt*. 2006; 45(30):7938–43. [PubMed: 17068531]
6. Komachi Y, Sato H, Aizawa K, Tashiro H. Micro-optical fiber probe for use in an intravascular Raman endoscope. *Appl Opt*. 2005; 44(22):4722–32. [PubMed: 16075885]
7. Hattori Y, Komachi Y, Asakura T, Shimosegawa T, Kanai G, Tashiro H, Sato H. In vivo Raman study of the living rat esophagus and stomach using a micro-Raman probe under an endoscope. *Appl Spectrosc*. 2007; 61(6):579–84. [PubMed: 17650367]
8. Matousek P, Clark IP, Draper ERC, Morris MD, Goodship AE, Everall N, Towrie M, Finney WF, Parker AW. Subsurface probing in diffusely scattering media using spatially offset Raman spectroscopy. *Appl Spectrosc*. 2005; 59(4):393–400. [PubMed: 15901323]
9. Matousek P. Inverse Spatially Offset Raman Spectroscopy for Deep Noninvasive Probing of Turbid Media. *Appl Spectrosc*. 2006; 60(11):1341. [PubMed: 17132454]
10. Matousek P. Deep non-invasive Raman spectroscopy of living tissue and powders. *Chem Soc Rev*. 2007; 36(8):1292–304. [PubMed: 17619689]
11. Stone NSN, Kerssens M, Lloyd GR, Faulds K, Graham D, Matousek P. Surface enhanced spatially offset Raman spectroscopic (SESORS) imaging - the next dimension. *Chem Sci*. 2011; 2(4):776–80.
12. Yuen JM, Shah NC, Walsh JT, Glucksberg MR, Van Duyne RP. Transcutaneous Glucose Sensing by Surface-Enhanced Spatially Offset Raman Spectroscopy in a Rat Model. *Anal Chem*. 2010; 82(20):8382–5. [PubMed: 20845919]
13. Buckley K, Matousek P. Recent advances in the application of transmission Raman spectroscopy to pharmaceutical analysis. *J Pharm Biomed Anal*. 2011; 55(4):645–52. [PubMed: 21112718]
14. Buschman HP, Marple ET, Wach ML, Bennett B, Schut TCB, Bruining HA, Bruschke AV, van der Laarse A, Puppels GJ. In vivo determination of the molecular composition of artery wall by intravascular Raman spectroscopy. *Anal Chem*. 2000; 72(16):3771–5. [PubMed: 10959962]
15. Schulmerich MV, Dooley KA, Vanasse TM, Goldstein SA, Morris MD. Subsurface and transcutaneous Raman Spectroscopy and mapping using concentric illumination rings and collection with a circular fiber-optic array. *Appl Spectrosc*. 2007; 61(7):671–8. [PubMed: 17697459]

16. Matousek P, Thorley F, Chen P, Hargreaves M, Tombling C, Loeffen P, Bloomfield M, Andrews D. Emerging Raman Techniques for Rapid Noninvasive Characterization of Pharmaceutical Samples and Containers. *Spectroscopy*. 2011; 26(3):44–51.
17. Michielsen K, De Raedt H, Przeslawski J, Garcia N. Computer simulation of time-resolved optical imaging of objects hidden in turbid media. *Phys Rep-Rev Sec Phys Lett*. 1998; 304(3):90–144.
18. Zonios G, Dimou A. Light scattering spectroscopy of human skin in vivo. *Opt Exp*. 2009; 17(3): 1256–67.
19. Ramachandran H. Imaging through turbid media. *Curr Sci*. 1999; 76(10):1334–40.
20. Cheong WF, Prah SA, Welch AJA. Review Of The Optical-Properties Of Biological Tissues. *IEEE J Quantum Electron*. 1990; 26(12):2166–85.
21. Kumari S, Nirala AK. Study of light propagation in human, rabbit and rat liver tissue by Monte Carlo simulation. *Optik*. 2011; 122(9):807–10.
22. Wilson RH, Mycek MA. Models of Light Propagation in Human Tissue Applied to Cancer Diagnostics. *Technol Cancer Res Treat*. 2011; 10(2):121–34. [PubMed: 21381790]
23. Jacques SL, Pogue BW. Tutorial on diffuse light transport. *J Biomed Opt*. 2008; 13(4):1–19.
24. Meresman H, Hudson AJ, Reid JP. Spectroscopic characterization of aqueous microdroplets containing inorganic salts. *Analyst*. 2011; 136:3487–95. [PubMed: 21373668]
25. Okagbare PI, Morris MD. Polymer-capped fiber-optic Raman probe for non-invasive Raman spectroscopy. *Analyst*. 2012; 137:77–81. [PubMed: 22059232]
26. Okagbare PI, Esmonde-White FWL, Goldstein SA, Morris MD. Development of non-invasive Raman spectroscopy for in vivo evaluation of bone graft osseointegration in a rat model. *Analyst*. 2010; 135(12):3142–6. [PubMed: 20924520]
27. Okagbare PI, Esmonde-White FWL, Goldstein SA, Morris MD. Transcutaneous Raman spectroscopy for assessing progress of bone graft incorporation in bone reconstruction and repair. *Proc SPIE*. 2011; 7883(78834I):78834I–1-I-8.

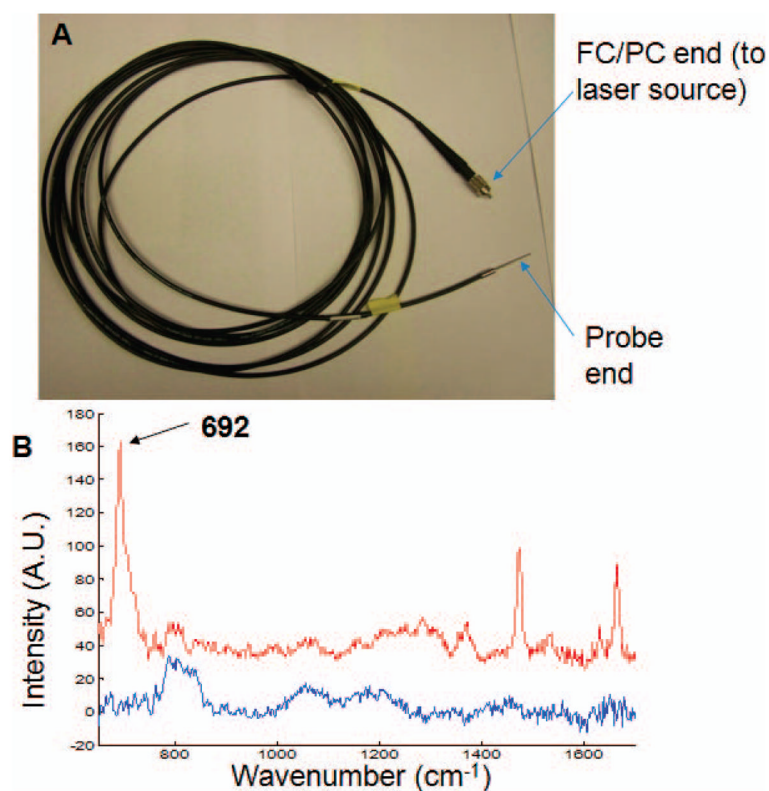


**Fig. 1.** (A) Cytop core excitation fiber with FC/PC connector for coupling to laser source and distal end stainless-steel ferrule for laser delivery to material under test. (B) Raman spectra of Cytop from a 5-m-long fluorocarbon fiber (red) and Raman spectra of silica from a 4-m-long silica core fiber (blue).

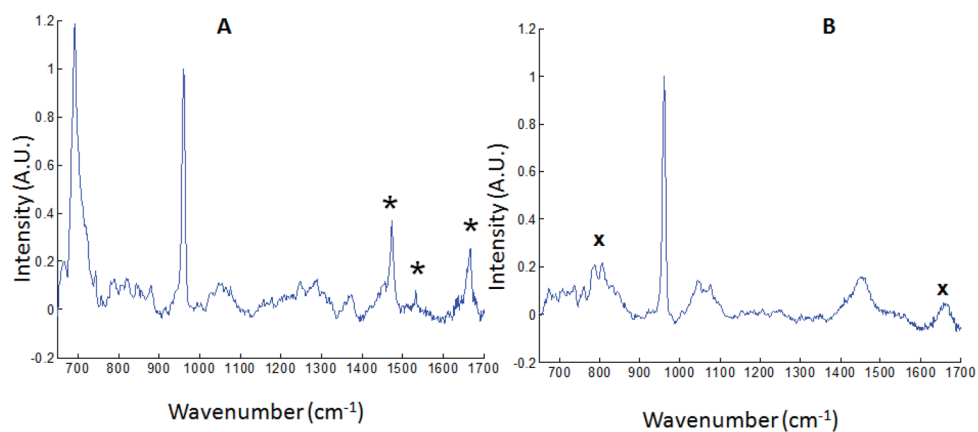


**Fig. 2.** Raman spectrum of rat tibia phantom with fluorocarbon excitation fiber, showing 692  $\text{cm}^{-1}$  reference band. Other bands from the fluorocarbon probe are marked with asterisks (\*). **(B)** Raman spectrum of the same phantom with silica excitation fiber. Both spectra are normalized to the HAP band at 960  $\text{cm}^{-1}$ . Bands due to silica background are marked with 'x'.

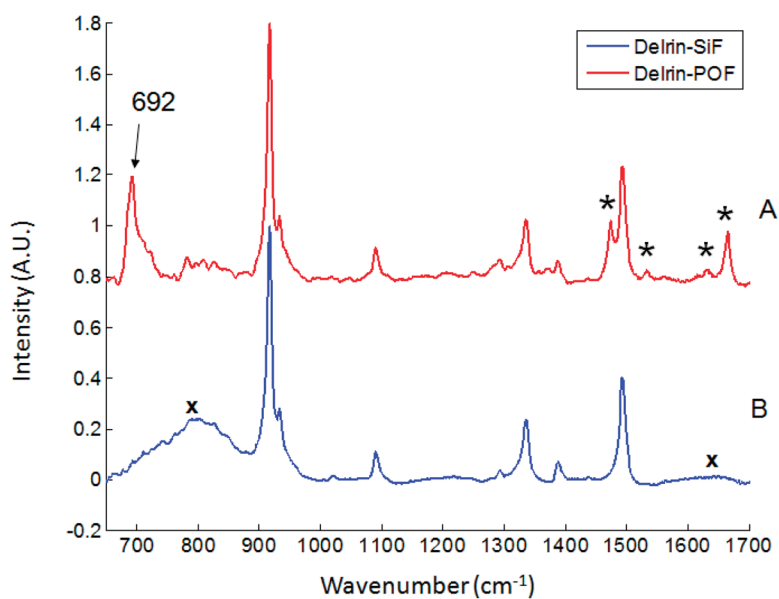


**Fig. 3.** (A) Raman spectrum of Delrin with fluorocarbon excitation fiber. Other bands from the fluorocarbon probe are marked with asterisks (\*). (B) Raman spectrum of Delrin with silica excitation fiber. Bands due to silica background are marked with 'x'.